Modulation Response of an Injection Locked Quantum-Dash Fabry Perot Laser at 1550nm

M. Pochet, N. A. Naderi, F. Grillot, N. Terry*, V. Kovanis*, L. F. Lester
Center for High Technology Materials, University of New Mexico
1313 Goddard SE, Albuquerque, NM 87106
*US Air Force Research Laboratory, 2241 Avionic Circle, WPAFB, OH 45433

ABSTRACT

The microwave domain modulation response of an injection-locked laser system is analyzed in the context of a Quantum Dash Fabry-Perot laser. This work demonstrates the applicability of a newly-derived modulation response function by using it to least-squares fit data collected on an injection-locked system with a Quantum-Dash Fabry-Perot semiconductor slave laser. The maximum injection strength, linewidth enhancement factor, coupled phase between the master and slave, and field enhancement factor characterizing the deviation of the locked slave laser from its free-running value are extracted by least-squares fitting the collected data with the function. The extracted values are then compared with theoretically expected values under the given detuning conditions. The correlation between the frequency of the resonance peak of the modulation response at the positive frequency detuning edge and a pole in the modulation response function under this detuning condition is illustrated. The calculation of the injection strength based on the experimental operating conditions is verified by applying the modulation response function to the experimental data. With the modulation response function, injection-locked behaviors can be accurately simulated in the microwave domain and used to predict operating conditions ideal for high-performance RF links.

Keywords: Injection-locked laser, quantum-dash, modulation response

1. INTRODUCTION

Injection-locking of semiconductor lasers has been shown to provide several improvements to directly-modulated lasers. These improvements include increasing the modulation bandwidth, suppressing nonlinear distortion, and reducing relative intensity noise, mode hopping, and chirp.[1-5] Various works found in the literature experimentally and theoretically analyze the physical mechanisms resulting in significant bandwidth and resonance frequency enhancement in injection-locked (IL) systems.[6-10]

This work's focus is to verify a derived small-signal modulation response function describing IL laser systems in the microwave domain. The modulation response function is used to describe a Quantum-Dash (QDash) Fabry-Perot (FP) slave laser that is injection-locked with a tunable single-mode external cavity master laser. This function represents a novel experimental approach facilitating the comparison of the relative magnitudes of the fitting parameters. The success of the least-squares fitting process requires the free-running operating parameters of the slave laser to be fully characterized in order to decrease the number of unknown parameters in the modulation response function. The free-running slave parameters carried forward and considered constant in the IL function include the free-running relaxation frequency and damping rate, the inverse differential carrier lifetime, and the parasitic carrier transport time. It is through the damping rate and relaxation frequency of the free-running slave laser that non-linear gain is included in the modulation response function. The extracted parameters characterizing the IL conditions include the maximum injection strength, linewidth enhancement factor, coupled phase between the master and slave, and field enhancement factor describing the deviation of the locked slave laser from its free-running value. Due to the function's multiple fitting parameters, there are many possible solutions that can fit the experimental data, thus requiring the extracted parameters to be properly restricted such that they can only vary in an acceptable fitting range. The extracted values are then compared with theoretical predictions and used to calculate the detuning frequency, which is compared to the experimentally observed value in order to validate the modulation response function. The frequency of the resonance peak of the observed modulation response at the positive frequency detuning edge is shown to correspond to a pole in the modulation response function. At the positive frequency detuning edge, one of the modulation response function's poles is dominated by the maximum injection strength, allowing for an approximation of the maximum injection strength value

to be extracted directly from the modulation response. Lastly, the maximum injection strength value extracted from the experimental data using the modulation response function is compared with the two common analytical methods used to calculate its value found in the literature.

The results show that under stable locking conditions the modulation response of a coupled IL system has a steady state solution that is well described with our modulation response function. This function can be used to extract operating parameters from the coupled system or to predict the maximum modulation bandwidth of an IL system given a constrained maximum available master laser power. Because the damping rate, relaxation oscillation frequency, linewidth enhancement factor, and output power of the slave laser vary with bias conditions for the QDash laser under study, the impact of their variation on IL behavior can be analyzed using the function.

2. THEORY

The small-signal modulation response function describing the IL laser system used here is derived from the fundamental rate equations described thoroughly in the literature.[1,2,6,8,11] When the operating parameters of the slave laser are known, the modulation response function can be used to extract the maximum injection strength, linewidth enhancement factor, coupled phase between the master and slave, and field ratio characterizing the deviation of the locked slave laser from its free running value of the coupled system by performing a least-squares fit of experimental modulation response data. Based on the extracted parameters, the threshold gain shift and the detuning frequency can be calculated. Additionally, the modulation response function incorporates the contribution of the inverse differential carrier lifetime, which proved to be relatively large for the FP QDash slave under study. The complete derivation of the response function is given by Naderi et al.[12] The modulation response function, $H_R(\omega)$, of a stably-locked IL system is described by the following equations:

$$|H_R|^2 = \frac{\left(\frac{C}{Z}\right)^2 (\omega^2 + Z^2)}{(C - A\omega^2)^2 + (B\omega - \omega^3)^2} \frac{1}{(1 + (\omega/\gamma_C)^2)} \tag{1}$$

$$A = (\gamma_{fr} - \gamma_N)R_{FE}^2 + \gamma_N + \gamma_{th} \tag{2}$$

$$B = \omega_r^2 + \gamma_N \gamma_{th} + \eta_O^2 / R_{FE}^2 + \gamma_{th}\left[(\gamma_{fr} - \gamma_N)R_{FE}^2 + \gamma_N\right] \tag{3}$$

$$C = (\eta_O / R_{FE})^2 \left[\gamma_N + (\gamma_{fr} - \gamma_N)R_{FE}^2\right] + (\omega_r^2 + \gamma_N \gamma_{th})Z \tag{4}$$

$$Z = (\eta_O / R_{FE})(\alpha \sin\varphi_O - \cos\varphi_O) \tag{5}$$

where ω_r, and γ_{fr}, are the free-running relaxation frequency, and free-running damping rate, respectively, and are known parameters from the free-running slave laser. γ_c is defined as $1/\tau_c$, where τ_c is the parasitic carrier transport time. γ_N is the inverse differential carrier lifetime. The injection strength, η, is defined as $\eta = \eta_O/R_{FE}$, where η_O is the maximum injection strength controlled by the experiment incorporating the coupling coefficient, fiber coupling efficiency, and the external power ratio of the experimental setup. η_O is also defined as $\eta_O = k_c(A_{inj}/A_{fr})$, where A_{inj} is the master laser field strength, A_{fr} is the free running slave field, and k_c is the coupling coefficient. The field enhancement factor, R_{FE}, takes into account the deviation of the steady-state field magnitude of the slave compared to its free-running value at high injection ratios[11], and is defined as $R_{FE} = A_O/A_{fr}$. The $[(\gamma_{fr} - \gamma_N)R_{FE}^2 + \gamma_N]$ term in (2) - (4) corresponds to the slave damping rate, γ_{slave}, under injection and is related to the free running damping rate and scales with the field enhancement factor. Thus, the field enhancement factor, R_{FE}, is used to scale free-running slave parameters under varied injection conditions. The correlation between the steady-state detuning phase offset and the linewidth enhancement factor is given by Z. The threshold gain shift, γ_{th}, and the frequency detuning, $\Delta f = f_{master} - f_{slave}$, are given by:

$$\gamma_{th} = 2(\eta_O / R_{FE})\cos\varphi_O \tag{6}$$

$$\Delta f = -\frac{\eta_O}{2\pi R_{FE}}\sqrt{1 + \alpha^2}\sin\left(\varphi_O + \tan^{-1}(\alpha)\right) \tag{7}$$

where α is the linewidth enhancement factor, and φ_O is the steady-state phase difference between the master and slave which is related to the detuning. The convention for the frequency detuning is defined as $\Delta f = f_{master} - f_{slave}$.

Analysis of the coupled system requires the operating parameters of the free-running slave laser to be known. First, the relaxation oscillation frequency, overall damping rate, and parasitic carrier transport time are determined by performing a least-squares fit on the free-running modulation response based on the standard model expressed as:[13]

$$|H_R|^2 = \frac{\omega_r^4}{\left((\omega_r^2 - \omega)^2 + \gamma_{fr}^2 \omega^2\right)\left(1 + (\omega/\gamma_c)^2\right)} \tag{8}$$

The slave laser damping rate plotted as a function of f_r^2 is used to extrapolate the value of the inverse differential carrier lifetime, γ_N. It is by implicitly incorporating the free-running slave laser parameters that non-linear gain is incorporated into the modulation response function through the K-factor given that $\gamma_{fr} = K f_r^2 + \gamma_N$.

The value of the coupling coefficient, k_c, is given by several methods found in the literature. Chrostowski[14] summarizes the methods, along with Lau.[15] The various approaches differ in how the injected field adds to the slave field. The calculation method most effective in matching the experimental data collected in this work is found to be given by:[15,16]

$$k_c = \frac{1}{\tau_i}\varepsilon_f = \frac{c}{2n_g L}\frac{(1-R)}{\sqrt{R}} \tag{9}$$

where τ_i is the internal round-trip time, ε_f is the field transmission coefficient[16], c is the speed of light in vacuum, L is the length of the laser cavity, R is the reflectivity of the emitting facet, and n_g is the group index. The derivation of the field transmission coefficient given in (9) is found in reference [15]. The field transmission coefficient accounts for the facet reflectivity in coupling the external field to the internal field. Assuming a reflectivity of 30% for a cleaved facet, the field transmission coefficient given in (9) is $(1-R)/\sqrt{R}$ = 1.26. An additional analytical means to calculate the field transmission coefficient uses $\sqrt{1-R}$ to account for the coupling of the fields[16], and its value is 0.84 given a reflectivity of 30%. The difference in the two calculation methods are notable, as they differ by a factor of ~1.5 and will therefore lead to a large change in the maximum injection strength for the case of FP lasers. The maximum injection strength, η_O, is determined using the coupling coefficient in (9) and is given by:

$$\eta_O = k_c \sqrt{\eta_c}\sqrt{P_{ext}} = \frac{c}{2n_g L}\frac{(1-R)}{\sqrt{R}}\sqrt{\frac{P_{master}}{P_{slave}}} \tag{10}$$

where η_c is the fiber coupling efficiency, P_{ext} is the external power ratio P_{master}/P_{slave}. P_{slave} is the total slave power measured using an integrating sphere in order to account for the total electric field within the laser cavity, and P_{master} is the power measured at the output of the fiber pigtail. The coupling coefficient is determined by comparing the slave power measured using the integrating sphere with the power coupled to the lensed fiber.

With the theoretical modulation response function described by (1) – (10), experimental data collected from an IL system can be lease-squares fit in order to extract α, φ_O, η_O, and R_{FE}. Due to the large number of possible solutions that will result from fitting experimental data with these parameters allowed to vary freely, constraints are applied to them such that they remain within reasonable limits. The constraints on the phase offset, φ_O, are based on the allowed locking range through the threshold condition, and show that the phase offset can vary from $-\pi/2$ for the positive frequency detuning edge to $\cot^{-1}(\alpha)$ for the negative frequency detuning boundary for stable locking. Based on the phase condition at the positive frequency detuning boundary, the value of the field enhancement factor, R_{FE}, will be equal to 1 since the slave's steady state field matches the free-running field due to the 90 degree phase offset between the master and slave. As the detuning frequency is decreased from the positive edge, the value of R_{FE} is greater than 1. The maximum injection strength, η_O, is constrained within an acceptable range from the value calculated using (9) & (10) and the value extracted directly from the modulation response at the positive frequency detuning edge as discussed in section 4. The value of the linewidth enhancement factor, α, is constrained closely to the value separately measured using the injection-locking technique.

The modulation response function can be used to predict the ideal operating conditions in order to achieve maximum modulation bandwidths of an IL system. Because the damping rate, relaxation oscillation frequency, and linewidth enhancement factor of the free-running slave laser are known to vary with bias conditions, their values must be optimized in order to maximize the modulation bandwidth. In a limitless situation a strongly biased slave laser could be injected with a very strong master laser signal in order to maximize the 3dB bandwidth; however, the master power

available is typically constrained. With this understanding, the function given can be used to explore the trade-offs between the operating conditions of the slave laser given a limited master laser power.

3. DEVICE AND EXPERIMENTAL SETUP

The experimental setup used is depicted in Fig. 1. The master laser was a New Focus 6200 external cavity tunable diode laser. The output of the master laser was fiber-pigtailed into a polarization maintaining (PM) single-mode fiber that was coupled into the second arm of a 3-port PM circulator. An erbium doped fiber amplified (EDFA), bandpass filter, and optical attenuator were available to be placed between the master laser and the input to port 2 in order to achieve high injection ratios when desired. The slave laser was coupled into port 1 of the circulator. The modulation response (S_{21}) was measured at port 3 of the circulator using an HP8722D network analyzer. An Ando AQ6317B optical spectrum analyzer, with a wavelength accuracy of 20 pm and wavelength linearity of 10 pm, was also connected to port 3 of the circulator and used to measure the detuning between the master and slave lasers, as well as determine conditions where the system was stably or unstably locked based on the side mode suppression ratio (SMSR) as the detuning and injected power were varied.
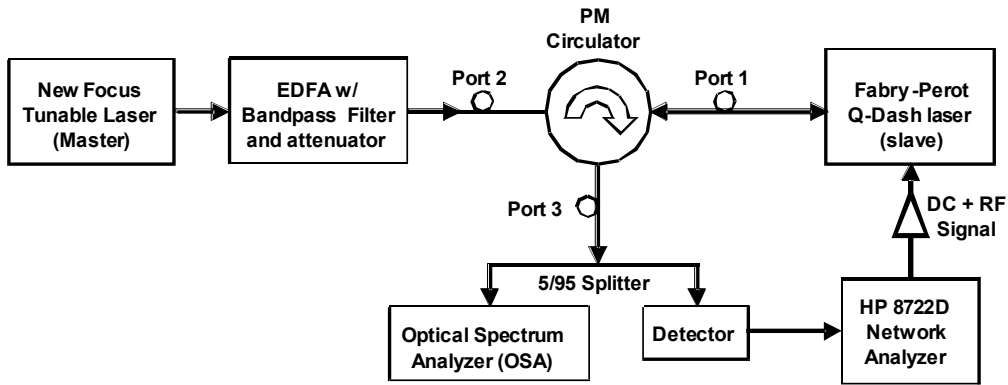

Fig. 1. Injection-locking experimental setup.

The slave laser was grown on an n^+-InP substrate. The active region consists of 5 layers of InAs quantum dashes embedded in compressively-strained $Al_{0.20}Ga_{0.16}In_{0.64}As$ quantum wells separated by 30 nm of undoped tensile-strained $Al_{0.28}Ga_{0.22}In_{0.50}As$ spacers. Lattice-matched $Al_{0.30}Ga_{0.18}In_{0.52}As$ waveguide layers of 105 nm are added on each side of the active region. The p-cladding layer is step-doped AlInAs with a thickness of 1.5 μm to reduce free carrier loss. The n-cladding layer is 500-nm thick AlInAs. The laser structure is capped with a 100-nm InGaAs layer. The lasers were designed to have four-micron wide ridge waveguides and 500 μm cleaved cavity lengths. The threshold current was measured to be 45 mA, with a slope efficiency of 0.2 W/A, and a nominal emission wavelength of approximately 1560 nm at room temperature.

4. ANALYSIS OF EXPERIMENTAL DATA

The modulation responses for a constant injection strength under varied frequency detuning values, along with the slave laser's free running response, are given in Fig. 2. The master laser's power was kept constant at 6.0 mW. The slave laser was biased at 60 mA DC, and the power coupled from a single facet was kept constant at 500 μW. Using the integrating sphere, 1.44 mW was measured from the slave at this bias making the fiber coupling efficiency, η_c, equal to 35% (P_{slave} = 2.88 mW). The slave laser's temperature was maintained at 20°C using a thermo-electric cooler. The 15.9 GHz (includes observed cavity mode shift, 11.3 GHz from free running value) and -20.8 GHz modulation responses represent the positive and negative stable frequency detuning boundaries, respectively, determined by measuring the SMSR on the optical spectrum analyzer as detuning is varied. Values of 30dB and 35dB SMSR are accepted values found in the literature.[15,16] Reference [14] notes the arbitrary nature of the threshold as it is typically determined by the experimentalist, while reference [15] discusses SMSR and relative intensity noise characteristics expected for stable and unstable behavior based on rate equation analysis, and states that 30 dB SMSR is required for stable locking. Fig. 2 also shows the least-squares curve fits of the data using the modulation response function given in (1) – (7). To perform

the curve fit, the free-running slave laser's operating parameters were extracted from the free-running modulation response model using (8), and the inverse differential carrier lifetime, γ_N, was determined by plotting the damping rate as a function of f_r^2.[18]
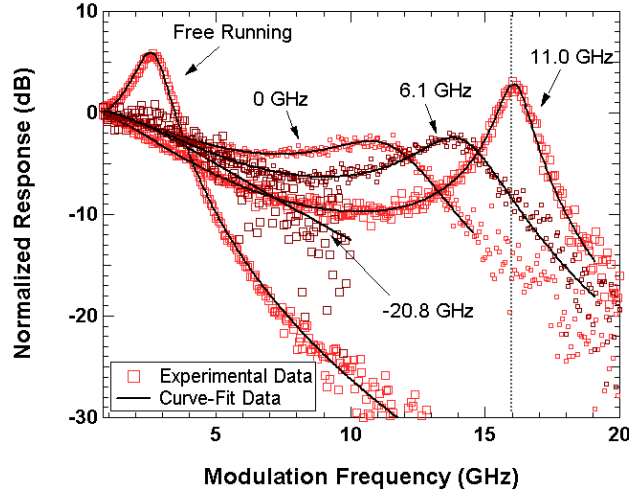

Fig. 2. Normalized modulation response of the free-running and the injection-locked laser under zero and extreme positive and negative frequency detuning conditions. The slave bias is 60 mA, with 500 μW coupled to the fiber. The master laser power is 6 mW. The frequency detuning value indicated on the figure is from the free running slave mode.

The value of the maximum injection strength can be approximated through inspection of the response at the positive frequency detuning edge. At this detuning frequency, the phase offset is -π/2 and R_{FE} is equal to 1 due to the 90 degree phase offset between the master and slave. The threshold gain shift is then equal to 0 (eqn. 6), and the expression for B in (3) is reduced to:

$$B = 4\pi^2 f_r^2 + \eta_O^2 \tag{11}$$

The significance of (11) is that $\sqrt{B}$ is directly proportional to the resonance peak frequency in the modulation response at the positive frequency detuning edge assuming that the free-running relaxation frequency is weak relative to the resonance peak frequency. With the value of B, the maximum injection strength, η_O, can be approximated. Therefore, it is seen that the resonance peak frequency in the modulation response at the positive frequency detuning edge is proportional in the order of terms to the maximum injection strength, as they increase and decrease together with a constant ratio.

In Fig. 2, the resonance peak for the 11.0 GHz detuning case (15.8 GHz when the cavity mode shift is considered) is observed at 16.0 GHz while the free-running relaxation frequency was previously extracted to be 2π·2.8 rad/s. Based on these values, η_O is calculated to be 93.2 GHz using (11). Given a cleaved facet reflectivity is of 30% and a measured group index of the active region of 3.5, η_O is calculated to be 99 GHz computed using (10), comparing well with the value extracted directly from the modulation response at the positive frequency detuning edge using (11). The injection strength was also calculated using other methods found in the literature to calculate the coupling coefficient; however, the approach given in (9) was found to be in the best agreement with the experimental data. The maximum injection strength, η_O, is therefore constrained to a range between 93.2 – 99 GHz when least-squares fitting modulation response data for frequency detuning values away from the positive frequency detuning edge.

Using (1) – (7) to least-squares fit the modulation response curves for the frequency detuning values under the injection strength given in Fig. 2 where P_{master} = 6mW, P_{slave} = 2.88 mW, and η_c = 35%, the values for α, φ_O, η_O, and R_{FE} were extracted and are given in Table 1. The free running parameters were determined to be: ω_r = 2π·2.8 rad/s, γ_{fr} = 8.1 GHz, and 6 GHz. The fitting results for the field enhancement factor, R_{FE}, increase from the positive frequency detuning edge (R_{FE} = 1) to the negative detuning edge. This trend corresponds to theory describing an increase in the slave laser steady-state power under negative detuning conditions and correlates as expected with the phase offset. The extracted phase offset results are consistent with the theory stating that stable locking varies from -π/2 at the positive frequency detuning

5

edge to $\cot^{-1}(\alpha)$ at the negative edge. The extracted linewidth enhancement factor values are consistent with those reported in reference [18] with respect to the accuracy of the method of measurement.

Table 1. Extracted operating parameters for the injection-locked condition shown in Fig. 2 (P_{master} = 6mW, P_{slave} = 2.88 mW, η_c = 35%).

Δf (GHz) (measured w/ cavity mode shift)	η_O (GHz)	α	ϕ_0 (rad)	R_{FE}	Calculated Δf (GHz)
11.0 (15.9)	99	2.8	-1.57	1	15.6
8.6	99	2.0	-1.45	1.08	10.9
6.1	99	2.1	-1.39	1.12	8.4
2.5	99	2.1	-1.31	1.19	5.8
0.0	94	2.15	-1.26	1.30	3.3
-7.4	94	2.9	-1.03	1.35	-7.5
-12.3	99	2.9	-0.841	1.42	-13.2
-20.8	99	1.9	+0.1	1.45	-21.7

Optical spectral responses for the various detuning conditions for the injection condition used in Fig. 2 are shown in Fig. 3. The free-running slave is shown in Fig. 3(a), indicating a Fabry-Perot mode separation of approximately 89 GHz. The master laser was locked to the mode centered at 1574.757 nm. The negative frequency detuning boundary demonstrated an abrupt change from locked state to unlocked state, shown in Fig. 3(b) (20 nm span) and Fig. 3(c) (0.5nm span). This abrupt change required monitoring a larger span than that shown in Fig. 3(c), as the injection conditions at –22.0 GHz observed using a 0.5 nm scan appeared to be stably locked with an SMSR of 32 dB. Fig. 3(b) shows the FP modes on the red-side of the master laser cease to be suppressed prior to the locked slave mode appearing as shown in Fig. 3(c). This is in stark contrast to the positive frequency detuning edge, shown in Fig. 3(d), where the detuning boundary is much less abrupt with the appearance of the slave mode slowly increasing as the detuning value is increased. The SMSR was measured to be -20, -30.2, and -38.1 dBm, for the 12.3 (16.5), 11.0 (15.9), and 9.8 (16.1) GHz detuning cases, respectively (cavity mode shift included in the calculation of detuning frequency). The significance of this gradual change from a locked state to an unlocked state draws to question the appropriate SMSR at which the system is considered effectively coupled together. Literature shows that the accepted SMSR is 30 or 35 dB to consider the system locked.[14,15] As the detuning is further reduced, the cavity mode is not observed due to its reduced amplitude and its obscurity in the noise floor.

A large shift in the cavity mode is exhibited in Fig. 3(d) and dictated by: $\Delta\omega = \Delta\omega_{inj} - \Delta\omega_{shift}$.[19] This shows that when using the function in (1) – (7) to determine ideal injection-locking conditions to maximize the 3dB bandwidth, the cavity mode shift phenomenon must be considered. This shift is also apparent in the modulation response at the positive frequency detuning edge, where the resonance frequency is equal to that of the detuning when the cavity mode shift observed in the optical spectrum is considered and not the detuning from the free-running slave. For improved curve-fitting results, the detuning frequency with consideration of the cavity mode shift is desired, which would allow for the values given in Table 1 to be more accurately compared with the actual detuning value. The data in Table 1 did include the cavity mode shift; however, it was only at detuning conditions close to the positive frequency detuning edge that the cavity mode was observed above the noise floor.

Additional cases where the extraction of the maximum injection strength from the modulation response and its comparison with corresponding values computed using (9) & (10) are illustrated in Fig. 4. In Fig. 4, the slave laser was biased at 70 mA, and 1 mW was coupled to the lensed fiber while 2.34 mW was measured from a single facet of the slave using the integrating sphere (P_{slave} = 4.68 mW). The master laser power was maintained at 4.5 mW and 7mW for the two cases shown. Again, the facet reflectivity was taken to be 30% and the group index 3.5. Using (9) & (10), the maximum injection strength, η_O, for the P_{master} = 4.5 mW case is calculated to be 70.0 GHz, which leads to a resonance peak at 11.1 GHz (70GHz/(2·π)). The expected value of the resonance peak is in strong agreement with the peak observed at the positive frequency detuning edge as illustrated in Fig. 4. For the P_{master} = 7.0 mW case the maximum injection ratio, η_O, is calculated to be 87.5 GHz using (10), leading to a resonance peak at 13.9 GHz. Again, the expected value of the resonance peak at the positive frequency detuning edge compares well with the experimentally observed value of 13.7 GHz.
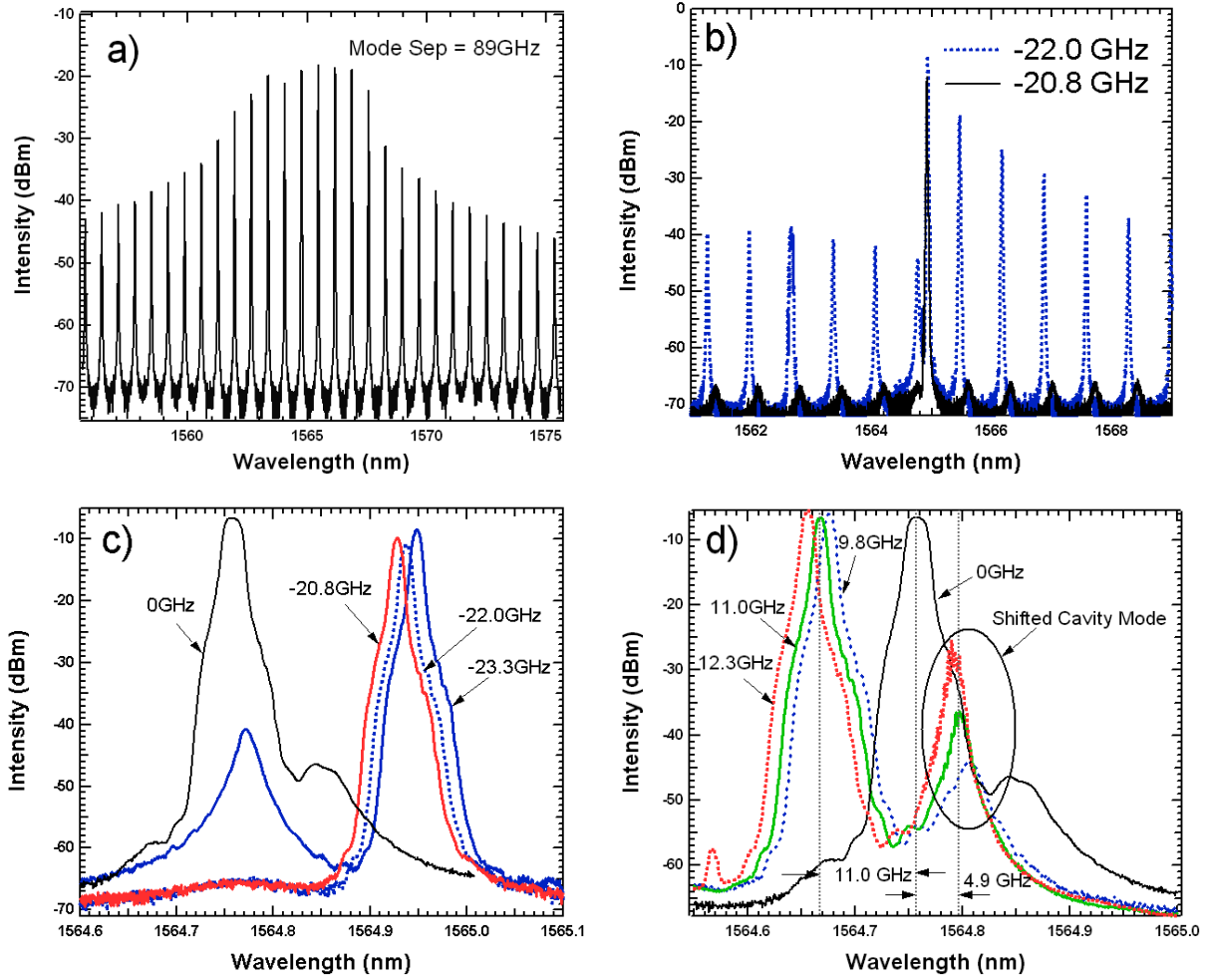
Fig 3. (a) Free-running slave. Negative frequency detuning progression to unlocked condition: (b) 0.5 nm span; (c) 20 nm span. (d) Positive frequency detuning progression to unlocked condition. The slave bias is 60 mA, with 500 μW coupled to the fiber. The master laser power is 6 mW.
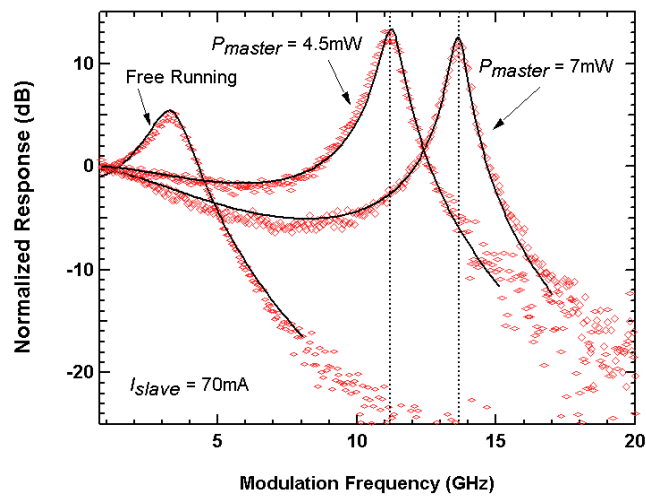

Fig. 4. Normalized modulation response of the free-running and the injection-locked laser at the positive frequency detuning edge. The slave bias is 70 mA, and P_{master} is varied for the two cases shown.

The extracted fitting parameters for the P_{master} = 7 mW case in Fig. 4 at the positive frequency detuning edge where Δf = 8.9 GHz (13.6 GHz with cavity mode shift accounted for) were: α = 2.7, φ_O = -1.5 radians , η_O = 85.3 GHz, and R_{FE} = 1.05. The free running parameters were determined to be: ω_r = $2\pi\cdot3.44$ rad/s, γ_{fr} = 9.8 GHz, and 6 GHz. The linewidth enhancement factor, α, at this bias current was previously measured to be 3.1, corresponding well with the extracted value. Thus, all values are in reasonable agreement with their expected theoretical magnitudes at the positive frequency detuning edge; however, the frequency detuning calculated using these values in (7) is 10.3 GHz where the expected value is 13.6 GHz, corresponding to the detuning with the cavity mode shift included. A second set of curve-fitting results for this injection strength resulted in the following parameter values: α = 1.1, φ_O = -1.56 radians , η_O = 86.3 GHz, and R_{FE} = 1.05, yielding a calculated frequency detuning value of 12.8 GHz which is in agreement with the expected value. These results yield a questionable value for the linewidth enhancement factor, α, which is smaller than the expected value measured using the injection-locking technique based on the asymmetry of the stable locking range[18]. Similarly, the extracted fitting parameters for the P_{master} = 4.5 mW case in Fig. 4 where the frequency detuning was 6.4 GHz (11.6 GHz with cavity mode shift accounted for) were: α = 2.7, φ_O = -1.47 radians, η_O = 68.1 GHz, and R_{FE} = 1.05. The primary change, as expected, between the two injection powers is the maximum injection strength, η_O, value. The downside of the extracted values is that the calculated frequency detuning value, 8.8 GHz, is less than the expected value of 11.6 GHz. It is noted that the extracted value of the phase offset, φ_O, differs from the expected value of $-\pi/2$ at the positive frequency detuning edge. Although the response was measured for a SMSR of 30dB, this extracted phase offset value indicates that the response was taken in the positive frequency detuning region, but not at the positive frequency detuning edge.

5. CONCLUSION

The curve-fitting results, when constrained by expected theoretical values, show that under stable locking conditions the modulation response function of coupled IL lasers has a steady state solution that is well described. This modulation response function can then be used to extract operating parameters from the coupled system, and to predict the maximum modulation bandwidth. Slave lasers ideal for injection-locking can be characterized in order to maximize modulation bandwidths by minimizing the sag in the modulation response when the IL system is under positive frequency detuning, which is shown in Fig. 2 to have the highest resonance frequency and hence the highest possible modulation bandwidth if the sag were to be reduced. The experimental data, along with the analytical modulation response function, was used to verify the calculation for the maximum injection strength for a FP slave laser. Because the damping rate, relaxation oscillation frequency, and linewidth enhancement factor of the slave laser are known to vary with bias conditions, the impact of the variations on the injection-locking behavior can be analyzed using the modulation response function. Lastly, the observations presented here show that QDash FP lasers are flexible transmitters capable of operating in high-performance RF links in that their operating characteristics (injection strength, detuning frequency, slave bias) can be manipulated to deliver a desired modulation response. With this flexibility they can be designed to have a high frequency resonance peak for bandpass operation or designed to have their pre-resonance sag stay above the -3dB point allowing them as operate in wideband transmitters.[20]

ACKNOWLEDGMENTS

REFERENCES

1. F. Mogensen, H. Olesen, G. Jacobsen, "Locking Conditions and Stability Properties for a Semiconductor Laser with External Light Injection," *IEEE Journal of Quantum Electronics*, Vol. QE-21, No. 7, pp. 784-793, 1985.
2. T. B. Simpson, J. M. Liu, A. Gavrielides, "Small-Signal Analysis of Modulation Characteristics in a Semiconductor Laser Subject to Strong Optical Injection," *IEEE Journal of Quantum Electronics*, Vol. 32, No. 8, pp. 1456-1468, 1996.
3. I. Petitbon, P. Gallion, G. Debarge, C. Ghabran, "Locking Bandwidth and Relaxation Oscillation of an Injection-Locked Semiconductor Laser," *IEEE Journal of Quantum Electronics*, Vol. 24, No. 2, pp. 148-154, 1988.
4. T. B. Simpson, J. M. Liu, "Enhanced Modulation Bandwidth in Injection-Locked Semiconductor Lasers," *IEEE Photonics Technology Letters*, Vol. 9, No. 10, pp. 1322-1324, 1997.
5. J. M. Liu, H. F. Chen, X. J. Meng, T. B. Simpson, "Modulation Bandwidth, Noise, and Stability of a Semiconductor Laser Subject to Strong Injection Locking," *IEEE Photonics Technology Letters*, No. 9, Vol. 10, pp. 1325-1327, 1997.

6.   E. K. Lau, H. K. Sung, M. C. Wu, "Frequency Response Enhancement of Optical Injection Locked Lasers," *IEEE Journal of Quantum Electronics*, Vol. 44, No. 1, pp. 90-99, 2008.

7.   E. K. Lau, X. Zhao, H. K. Sung, D. Parekh, C. Chang-Hasnain, M. C. Wu, "Strong optical injection-locked semiconductor lasers demonstrating > 100-GHz resonance frequencies and 80-GHz intrinsic bandwidths," *Optics Express*, Vol. 16, No. 9, pp. 6609-6618, 2008.

8.   L. Chrostowski, B. Faraji, W. Hofmann, M. C. Amann, S. Wieczorek, W. W. Chow, "40 GHz Bandwidth and 64 GHz Resonance Frequency in Injection-Locked 1.55 µm VCSELs", *IEEE Journal of Selected Topics in Quantum Electronics*, Vol. 13, No. 5, pp. 1200-1208, 2007.

9.   A. Murakami, K. Kawashima, K. Atsuki, " Cavity Reponance Shift and Bandwidth Enhancement in Semiconductor Lasers with Strong Light Injection," *IEEE Journal of Quantum Electronics*, Vol. 39, No. 10, pp. 1196-1204, pp. 043804-1-9, 2003.

10. A. Murakami, "Phase Locking and Chaos Synchronization in Injection-Locked Semiconductor lasers," *IEEE Journal of Quantum Electronics*, Vol. 39, No. 3, pp. 438-447, 2003.

11. A. Murakami, K. A. Shore, "Analogy between optically driven injection locked laser diodes and driven damped linear oscillators," *Physical Review A*, 73, 2006.

12. N. Naderi, M. Pochet, F. Grillot, N. Terry, V. Kovanis, L. F. Lester, *J. Special Topics in Quantum Electronics*, submitted Oct 2008.

13. P. Bhattacharya, D. Klotzkin, O. Qasaimeh, W. D. Zhou, S. Krishna, D. H. Zhu, "High speed modulation and switching characteristics of InGaAs-AlGaAs self-organized quantum dot lasers," *IEEE Journal of Selected Topics in Quantum Electronics*, Vol. 6, pp. 426-438, 2000.

14. L. Chrostowski, "Optical Injection Locking of Vertical Cavity Surface Emitting Lasers," *PhD Dissertation*, UC Berkeley, Spring 2004.

15. E. K. Lau, "High-Speed Modulation of Optical Injection-Locked Semiconductor Lasers," *PhD Dissertation*, UC Berkeley, Dec 2006.

16. H. Li, T. L. Lucas, J. G. McInerney, M. W. Wright, and R. A. Morgan, "Injection locking dynamics of vertical cavity semiconductor lasers under conventional and phase conjugate injection," *IEEE Journal of Quantum Electronics*, vol. 32, pp.227-35, pp. 227-235, 1996.

17. N. Schunk, K. Petermann, "Noise Anslysis of Injection-Locked Semiconductor Injection Lasers," *IEEE Journal of Quantum Electronics*, Vol. QE-22, No. 5, pp. 642-650, 1986.

18. F. Grillot, N. A. Naderi, M. Pochet, C.-Y. Li and L. F. Lester, "Variation of the feedback sensitivity in a 1.55µm InAs/InP quantum-dash Fabry-Perot semiconductor laser," *Applied Physsics Letters,* 93, pp. 191108, 2008.

19. T. B. Simpson, J. M. Liu, K. F. Huang, K. Tai, C. M. Clayton, A. Gavrielides, V. Kovanis, "Cavity enhancement of resonant frequencies in semiconductor lasers subject to optical injection," *Physical Review A*, Vol. 52, No. 6, pp. R4348-R4351, 1995.

20. R. C. Williamson, R. Esman, "RF Photonics," *IEEE Journal of Lightwave Technology*, Vol. 26, No. 9, pp. 1145-1153, May 2008.